A 4-meter, Wide Field Coronagraph Space Telescope for general astrophysics and exoplanet observations

Domenick Tenerelli[a], Roger Angel[b], Jim Burge[b], Olivier Guyon[c], Ann Zabludoff[b], Ruslan Belikov[d], Eugene Pluzhnik[d,] Robert Egerman[e]
[a]Lockheed Martin Space Systems, [b]University of Arizona, [c]University of Arizona, Subaru, [d]ARC-SSA, [e]ITT

ABSTRACT

The Wide Field Coronagraph Telescope (WFCT) is a 4-meter space telescope for general astrophysics and exoplanet observations that meets the 2000 Decadal Committee requirements.

This paper presents a design for a 4-m diameter, off-axis space telescope that offers high performance in both wide field and coronagraphic imaging modes. A 3.8 x 3.3-m unobstructed elliptical pupil is provided for direct coronagraphic imaging of exoplanets and a 4-m diameter pupil for wide-field imaging from far-ultraviolet (UV) to near-infrared (IR). The off-axis wide-field optics are all reflective and designed to deliver an average of 12 nm wavefront aberrations over a 6 x 24 arcminute field of view (FOV), therefore providing diffraction-limited images down to 300 nm wavelength and 15 mas images down to a wavelength limit set only by the mirror coatings. The coronagraph with phase-induced amplitude apodization (PIAA) provides diffraction suppression around a 360-degree field with high Strehl and sensitivity at the 1e-10 level to an inner working angle of 2 λ/D (or 50 mas at 500 nm wavelength).

This paper focuses on the optical design that allows the above imaging features to be combined in single telescope, and gives a preliminary spacecraft design and costing, assuming a distant trailing orbit.

Keywords: 4-meter, astrophysics, coronagraph, exoplanet, off-axis, telescope, wide-field

1. INTRODUCTION

The science case and possible instrument suite are based on other more detailed mission concept studies in which several of the authors have participated. The goal of this paper is to introduce a novel technical approach for the telescope and to explore its scientific potential, rather than report on a well-established, ongoing mission study. Although compatibilities between instrument optical designs and our telescope design were not explored in detail or modeled, preliminary analysis suggests it will be valuable to NASA to explore this option, along with alternative imaging and coronagraphic solutions, or use of an external occulter.

The WFCT mission concept is inspired from, and makes extensive use of, technologies and instrument concepts that have been developed by several groups. Significant recent advances (from theory to lab validation) in coronagraphy and wavefront control, performed at NASA centers and several U.S. universities, are incorporated.

The Pupil Mapping Exoplanet Coronagraphic Observer (PECO) instrument, developed with NASA JPL and NASA Ames, is similar to the PIAA coronagraph instrument for WFCT, and the exoplanet science case is extrapolated from the PECO report. A summary of the Ames coronagraph testbed is also provided. The ongoing study of the application of WFCT/PIAA to high-precision mass measurement of exoplanets is summarized. The WFCT wide-field instruments are based on designs developed in detail for the Telescope for Habitable Exoplanets and Intergalactic/Galactic Astronomy (THEIA) mission concept studies. Additional studies exploring how coronagraphy and general astrophysics can be combined in a single mission were carried out for the Terrestrial Planet Finder-Coronagraph (TPF-C) flight baseline 1. Confidence in the practicality of the WFCT off-axis telescope is based on recent advances in metrology enabling manufacturing of large off-axis telescopes with little additional risk and cost compared to on-axis telescopes. Use of emerging technologies in vibration isolation and laser communications, which enable the construction of a large telescope with sufficient stability for high contrast coronagraphic imaging, are also envisioned.

WFTC is a flagship class mission. The team estimates a lifetime cost of $4.2B, including $3.3B for development: $1.4B for the telescope, $700M for the instruments, and a $900M development reserve.

Space Telescopes and Instrumentation 2010: Optical, Infrared, and Millimeter Wave,
edited by Jacobus M. Oschmann Jr., Mark C. Clampin, Howard A. MacEwen, Proc. of SPIE
Vol. 7731, 77311N · © 2010 SPIE · CCC code: 0277-786X/10/$18 · doi: 10.1117/12.860719

2. SCIENCE OVERVIEW

2.1 WFCT Science Summary

Over the past 25 years, the Hubble Space Telescope (HST) has revolutionized our view of the universe, excited and engaged the general public with its compelling images of the universe, and has been a workhorse for astrophysics. As a worthy successor to HST and companion to the James Webb Space Telescope (JWST), it is proposed that NASA build the Wide Field Coronagraph Telescope (WFCT), a flagship-class mission with a 4-meter primary mirror, featuring a visible and UV imager with an exceptionally wide field, a high resolution far-UV spectrograph, and an optimized coronagraph eminently capable of detecting, imaging, and spectroscopically characterizing terrestrial-class exoplanets.

WFCT will be capable of addressing many of the most important questions in astronomy: Are we alone? Are there other habitable planets? How frequently do solar systems form and survive? How do stars and galaxies form and evolve? How is dark matter distributed within and between galaxies? Where are most of the atoms in the universe? How were the elements necessary for life created and distributed through cosmic time?

2.2 WFCT Instrument Capabilities

The WFCT telescope design is an off-axis three-mirror anastigmat (TMA), with a 4-meter MgF coated primary mirror (PM), a LiF-coated secondary mirror (SM), and three main instruments: (1) the wide field imager (WFI), a dual-channel, wide-field UV and optical imager covering 6 x 24 arc-minutes on the sky with 18 milli-arc-second (mas) pixel scale and spectral sensitivity from 120–1100 nm, to be resolved (TBR); (2) a multipurpose far UV spectrograph (UVS) optimized for high sensitivity observations of faint astronomical sources at spectral resolutions R/30,000–100,000 in the 1000–3000 Å band; and (3) the Phase Induced Amplitude Apodization Coronagraph (PIAAC) instrument (Guyon, 2003), with four narrow-field cameras, dividing the observation band from 200–1200 nm (TBR), and an R/70 integral field spectrograph (IFS).

2.3 WFCT Mission Considerations

Both ground and space systems extensively leverage heritage equipment, processes, and procedures. The mission is developed by an experienced team including ARC, LM, UA, and ITT. The key mission parameters are given in Section 4.0. The Optical Telescope Assembly (OTA) is detailed in Section 5.0, and the science instruments (SI) are described in Section 6.0. The spacecraft design is discussed in Section 7.0.

The major challenges for the WFCT mission are: (1) fabricating a 4-meter telescope that is diffraction-limited at 300 nm; (2) fabricating the large required focal plane arrays; and (3) fabricating and correcting the PIAA coronagraph optics to the required level. Well-defined, realizable solutions exist to these challenges; however, the mission will require technology development.

2.4 Astrophysical Rationale for WFCT

The large-aperture UV and optical wavelength telescope proposed for WFCT is wide-field, diffraction-limited, point spread function (PSF), stable, and clearly an all-purpose facility and a necessary complement to JWST. The case for such a mission has been made in many previous documents, including the proposal for THEIA (Kasdin, 2009), the original concept that provides a foundation for the new design presented here. Unlike THEIA, the off-axis/coronagraph design of WFCT *eliminates the need for a companion occulting satellite.*

Given that dramatic technical advances have made tractable the stringent wavefront control requirements for coronagraphy and reduced the costs of off-axis mirrors, the current mission design provides a less complex and potentially lower cost path to the exciting science described in the THEIA white paper. Furthermore, the three principal THEIA instruments can be adapted to fit to the WFCT OTA and will easily fit in the WFCT telescope bay. Several additional scientific programs that require the wide-field, high spatial resolution and PSF-stable characteristics of WFCT are highlighted below. Like HST, many of most important discoveries will likely be unanticipated.

2.5 History of the Local Volume

The star formation history of galaxies can be reconstructed from detailed synthesis of stellar color magnitude diagrams (CMDs) (cf. Harris & Zaritsky, 2004). Such a program is under way using HST, and the variety and detail of the CMDs is manifest, as shown in Figure 2.5-1. The CMDs can be used to reconstruct the history of each galaxy and of the overall

volume. WFCT will have several advantages over current baselines: (1) larger FOV; (2) supreme PSF stability with ~two times sharper PSF; and (3) increased aperture.

Many of the nearby galaxies have optical sizes exceeding a few arc-minutes, and the stellar halos of these galaxies have recently been found to extend much farther than the "optical size." The Large Magellanic Cloud halo is at least a factor of two larger than the classical size, and perhaps even much larger (Munoz et al, 2006). Streamers are found in M 31 to ~five larger radius than the size of its disk (Ibata et al, 2007). The halos of these galaxies are particularly interesting in constraining the oldest populations and in uncovering the relics of their presumably tumultuous growth; therefore FOV is critical.

The photometry is typically limited by crowding rather than by photon noise. As such, these types of analyses rely on PSF fitting and subtraction of nearby neighbors. A diffraction-limited PSF is key, but so is PSF stability, so that the modeling is highly constrained.

Finally, the gain in aperture size provides both reduced PSF and increased light-gathering capability, with a gain following the fourth power of the increased diameter, which is particularly applicable in the outer galactic regions that are not crowding-limited. The current program includes ~70 galaxies within 4 Mpc, but is incomplete and barely reaches other nearby groups of galaxies. By going somewhat further, we gain both in the range of environments explored and in the number of giant galaxies available, both of which are key to obtaining a truly representative reconstructed history of the star formation in the universe.

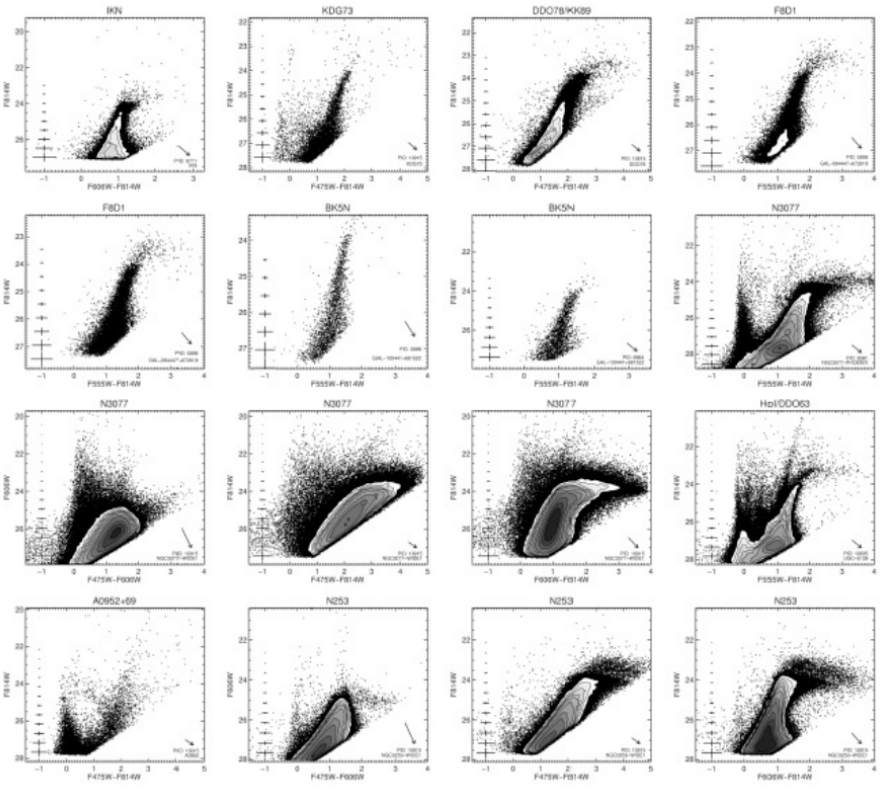

Figure 2.5-1. Sixteen example CMDs from the ANGST survey

2.6 The Nature of Dark Matter

Until dark matter is detected in the laboratory, study of most of the matter in the universe is limited to indirect measurements in astrophysical settings. Until recently, the measurements of dark matter on galaxy and cluster scales were also fit with relatively simple ad hoc variations of gravity. The discovery and study (Clowe et al, 2006) of the colliding Bullet Cluster, shown in Figure 2.6-1, made the case for much stronger dark matter, since the mass, as traced by gravitational lensing, was found to be displaced from the dominant baryonic component (the hot gas). Clusters are

particularly useful for dark matter studies, because they are the one environment in which nearly all of the baryons are accounted for (therefore the dark matter and missing baryon problems are decoupled). WFCT provides a sharp and stable PSF and high sensitivity, which is ideal for high-precision weak lensing measurements.

A second result of the Clowe et al study was the measurement of an upper limit on the self-interaction cross-section of dark matter. The precision of this measurement is currently limited by the relative centroiding of the galaxy distribution and weak lensing signals. With deep, diffraction limited imaging over wide fields, it is possible to go further down the luminosity function to increase the number of cluster galaxies identified and also improve weak lensing maps. Furthermore, such imaging should also reveal a sea of strongly lensed images that can be used jointly with the weak lensing to remove the mass-sheet degeneracy (Bradac et al, 2008) and examine the central dark matter profile, which itself can constrain the self-interaction strength of dark matter.

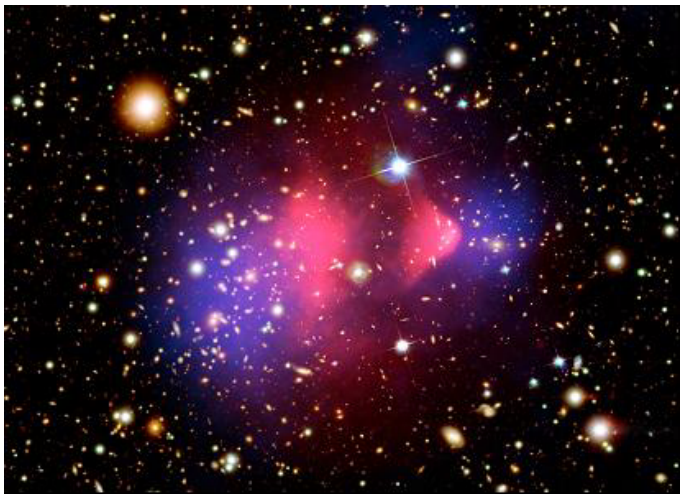

Figure 2.6-1. The Bullet Cluster. Blue shows mass distribution (from weak lensing) and pink shows X-ray emitting plasma. The displacement proves dark matter is not simply the incorrect calculation of the gravitational potential due to baryons.

2.7 Galactic Mass Accretion

Galaxies grow partly by accretion of gas from the surrounding intergalactic medium and partly by mergers with other galaxies. Observational studies of galaxy assembly have focused primarily on merger rates, which can be measured indirectly by counting close pairs and merger remnants of galaxies. However, all the mass that enters the galaxy population ultimately does so by accretion—mergers can only redistribute this mass from smaller systems to larger systems (Keres et al, 2004). Identifying the signatures of this accretion would be a significant step in our understanding of how galaxies form.

Recent simulations of galaxy formation predict that gas being accreted by young galaxies channels some of its gravitational cooling radiation into atomic emission lines such as hydrogen Lya (1216 A; Haiman, Spaans & Quataert, 2000; Fardal et al, 2001). These predictions have coincided with the discovery of the so-called “Lya blobs,” mysterious, extended sources in the distant universe with typical sizes of 10–20 arcsec and Lya line luminosities of ~10^44 erg/s (e.g., Keel et al, 1999; Steidel et al, 2000; Francis et al, 2001; Dey et al, 2005; Yang et al, 2009). While the emission from these blobs could be cooling radiation, it could also arise from other sources, including collisionally ionized gas in galactic superwinds (Taniguchi & Shioya, 2000) or gas photoionized by young stellar populations or by active galactic nuclei.

Attempts to isolate the origin of blob emission and their likely end-products have foundered due to several factors. First, the few known Lya blobs have been found in non-random, clustered fields, so it is difficult to assess how representative these samples are and to compare them directly with gas accretion simulations, which are best at modeling random patches. Second, the relationship between these extended Lya sources and more numerous, compact, Lya-emitting galaxies is muddled by our inability to detect an intermediate population of fainter, moderately extended sources in ground-based seeing. Third, the properties of Lya sources are even less understood at redshifts below 2, because of the inaccessibility of the Lya line from the ground.

The large aperture, wide-field, PSF-stability, and diffraction-limited capability of WFCT makes it possible to conduct blind and thus representative surveys for the full range of Lya sources, including hundreds of Lya blobs and tens of thousands of compact emitters. With a narrow- or medium-band filter set, a wide-field UV/optical imager on WFCT could detect these sources in a consistent manner from the current epoch to redshifts of 8.

2.8 Planet Detection and Characterization

WFCT will directly image planetary systems of nearby stars in visible light with spectral resolution $R = \lambda/d\lambda = 70$. It will have the sensitivity to detect Earth-like rocky planets at in habitable zones and to spectrally characterize their surfaces or atmospheres. WFCT can detect small (1–2 Earth radius) and giant planets, as well as circumstellar disks with high spatial resolution (~25 mas) and high contrast (~1e-10), as close as $2\lambda/D$ (50 mas at 500 nm) from host stars. WFCT will produce R=70 images in up to over the 200–1200 nm (TBR) wavelength range.

With a 3.8 x 3.3 meter unobstructed elliptical pupil, combined with the high throughput, low IWA PIAA coronagraph, WFCT is well suited to characterize a large number of exoplanets and disks. The science case for exoplanet imaging and spectroscopy with a 4-m class telescope was previously formulated by the THEIA team; only the key highlights are given here.

High SNR images from WFCT of nearby exoplanetary systems will allow unambiguous identification of Earth mass exoplanets and disk features, and will have sufficient resolution for orbit determination. Figure 2.8-1 shows simulated four- hour exposures of a Sun + Earth + Exozodi system at 8.7 pc (top) and 4.35 pc (bottom) in the 500nm–600nm bandpass with a 25% efficiency.

WFCT can identify Earth-like planets around a large number of stars. In the 500–600 nm band alone, SNR = 7 detection of a candidate planet is achieved in under 10 hours integration (with 25% efficiency and maximum elongation), for more than 50 stars.

WFCT has the sensitivity to characterize the atmospheres of several Earth-like planets and potentially provide evidences of life. At 550 nm, there are 20 stars for which WFCT can acquire a R = 50 spectrum, at SNR = 10, with under 24-hour integration. The number of such “high sensitivity” stars decreases as wavelength increases.

The major PIAAC Planet Finding Goals are: (1) to conduct a “Grand Tour” of the habitable zones of many nearby stars, searching for Earth and Super-Earth planets, and visit each target multiple times for possible detections; (2) to characterize detections and measure spectral features by integrating to S/N = 20–30: (3) to detect known radial velocity planets (RVPs) with single visits at maximum elongation, observe RVPs by integrating to S/N >30, and obtain spectral features; and (4) for exozodiacal disks and gas giants to obtain a snapshot survey of several hundred nearby stars, study diversity of dust disks, and search for gas giant planets.

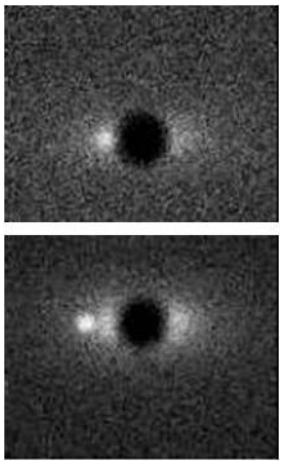

Figure 2.8-1. PIAAC detection of a Sun + Earth + Exozodi system

2.8-1 High Precision Mass Measurement of Expoplantes

Initial results (Guyon, Shao, Shaklan et al, 2010) indicate that WFCT allows simultaneous coronagraphic imaging of exoplanets and deep imaging of a wide field around the coronagraphic field. The astrometric signal can be detected as a shift between background stars and a central star. Referencing between two fields is provided by small dots on the primary mirror.

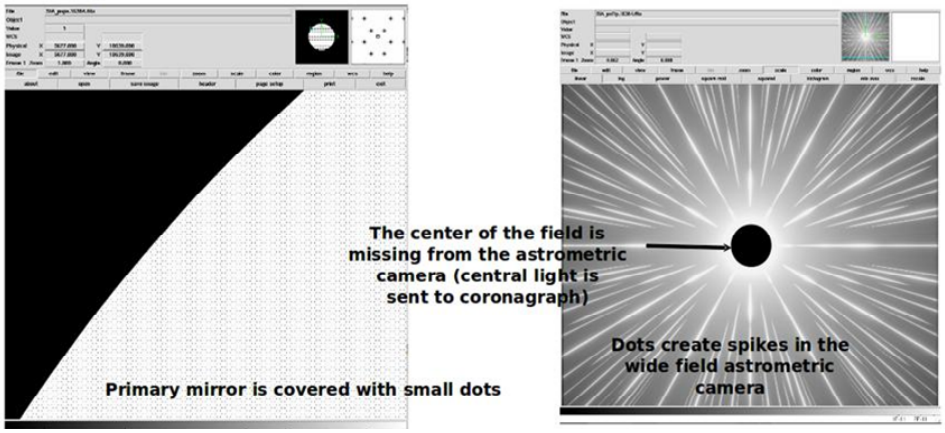

Fig. 2.8.1-1 Dots on primary mirror create a series of diffraction spikes used to calibrate astrometric distortions.

3. TECHNICAL OVERVIEW & MISSION REQUIREMENTS

The WFCT spacecraft will be a Spitzer heritage vehicle flown on a Delta-II launch vehicle, and the spacecraft will launch into an Earth-trailing, drift-away heliocentric orbit, with the required stable thermal environment, similar to the Spitzer orbit. The low launch energy allows for significant mass savings over other orbit options. The spacecraft design is described in Section 7.0. A CAD model of the observatory is shown in Figure 3-1. Mission requirements are given in Table 3-1.

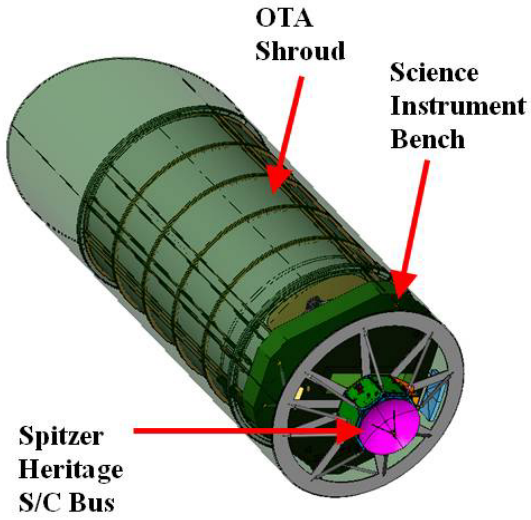

Figure 3-1 4-m WFCT Configuration

Table 3-1. Mission requirements

Lifetime	5 yrs (10 yrs goal)
Launch date	Oct 1, 2019
Orbit altitude	Earth trailing
SC-Earth Distance	0.6 AU
Epoch Time	30 days from launch
C3 Energy	0.4
P/L Mass	427 kg
Optics Temp	270±10K
Focal Plane Temp	150±2K
P/L Power (EOL)	1430 W
Downlink	30 Mbps at 0.6 Au
Uplink	2 kps
Data Storage	40 Gbytes
Ground Contact	2-2 hr/ week
Fine Pointing	0.1 arc-secs
Coarse Pointing	3 arc sec
Jitter/Stability	<1milli arc-sec
Fine Guidance	P/L to provide to spacecraft
Sun Avoidance	60 deg
Radiation	20 krad
Launch vehicle	Delta IV / Atlas V
Safe Mode System	Autonomous Safing

3.1 Optical Telescope Assembly (OTA) Design

The OTA is a three-mirror anastigmat (TMA) design provided by Jim Burge, University of Arizona. It has an off-axis primary mirror, optimized for a very wide field of view (24 x 6 arcmin) and a system focal length for the baseline design of 64 meters. The corresponding plate scale is thus 319 microns/arcsec, or 32 mas per 10-micron detector pixel. The primary mirror (PM) shape is that of a portion of a 7.7-m diameter f/0.9 on-axis parent. The secondary mirror (SM) is

offset, resulting in a 3.8 x 3.3 m unobscured elliptical pupil. The OTA fits within a cylinder 4-m in diameter and 8-m long (acceptable for Delta-II 5-m fairing).

Figure 3.1-1 shows the OTA ray-trace.

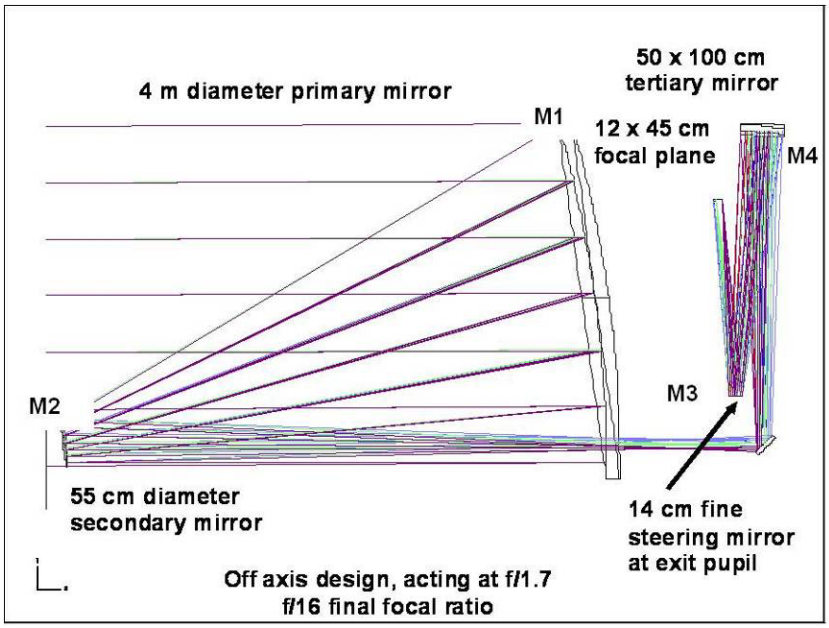

Figure 3.1-1. OTA Ray-Trace for WFCT TMA Design

The WFE is less than 10 nm rms over most of the 6 x 24 arcmin field, and averages only 12 nm rms over all the field. Thus the image quality results in excellent diffraction-limited images down to 300 nm wavelength, and 15 mas images at shorter wavelengths down to a wavelength limit set only by the mirror coatings. The mean imaging distortion is < 0.4%. See Figure 3.1-2.

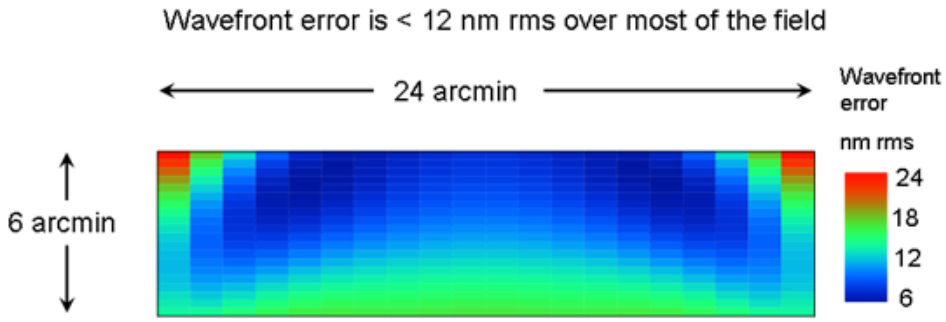

Figure 3.1-2. Wavefront aberration in nm rms over the 6 x 24 arcsec FOV

A fine steering mirror (FSM) is located at the system exit pupil. The field curvature corresponds to a 2.2 m ROC, and the field curvature is concentric with the fine steering mirror at the stop, allowing for a large field of regard for FSM motion. FSM motion could also allow switching between instruments, each of which would have access to the full 6 x 24 arcmin FOV.

Alternate designs with longer focal length to better match pixels to the UV diffraction limit are also possible and are being developed. For example, a design 100 m focal length yields 10 micron pixels of 21 mas.

The selected optical telescope assembly (OTA) design for WFCT is highly leveraged from the recently launched 1.1-meter high resolution NextView Electro-Optical payload developed by ITT. This approach maximizes the use of high TRL hardware and proven design and manufacturing processes.

The optical prescription was selected to be off-axis to prevent diffraction from any obstructions (ee Figure 3.1-3). To maximize the amount of light collection, a unique optical design was developed, in which the SM only slightly obstructs a region of the PM for a strongly concentrated diffraction pattern only slightly degraded from the classical Airy pattern. The 4-meter off-axis system will be packaged in a standard 5-meter diameter shroud fairing. This concept also allows for a long stray light baffle to extend forward from the PM's metering structure towards the SM.

The off-axis nature of the OTA, compared to an on-axis design, does introduce additional technical complexities. However, technology developments over the last 15 years in terms of optical processing, metrology, and alignment techniques enable off-axis systems to be made with only small impacts to cost, schedule, and risk.

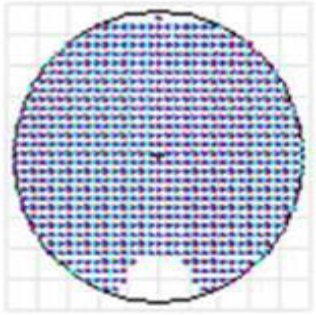

Figure 3.1-3. A 4-m wide-field pupil, showing very small obscuration

3.2 OTA Mechanical Design

The PM and SM will be fabricated out of Corning Ultra Low Expansion (ULE®) glass for its excellent thermal stability characteristics around room temperature. A mechanical design has been developed for the PM, which is manufacturable utilizing today's technology. The mirror blank comprises a segmented abrasive water jet weight core with hexagonal cells that is fused to monolithic facesheets. The design has global and local stiffnesses that are comparable to optics ITT has polished in the past with similar requirements (global stiffness relates to the first flexible mode, and local stiffness relates to the gravity deflection of the unsupported regions of the optical surface).

The OTA precision metering structures coupled with a fairly simple thermal control system are able to keep the optics in alignment to the required tolerances. The precision metering structures are fabricated using fibers and a state-of-the-art cyanate siloxane resin system (co-patented by ITT). ITT's experience in using these materials results in metering structures that have thermal stability on the same order of magnitude as ULE® glass with nearly negligible hygroscopic effects.

The OTA is surrounded by a monolithic outer barrel assembly (OBA), which is scarfed at 45° to minimize stray light effects. The OBA is also integral to the thermal control system, and science instrument radiators may be mounted to it. The OBA will also have a contamination cover to maintain OTA cleanliness throughout ground test and launch.

3.3 WFCT Science Instrument Descriptions

The WFCT science payload is currently conceived as having three science instruments: a wide field imager (WFI), UV spectrograph (UVS), and Phase Induced Amplitude Apodization Coronagraph (PIAAC).

The PIAAC instrument is considered first, with the interface to the OTA, in Section 6.1, and a summary of instrument capabilities in Section 6.2. The UVS and WFI instruments are considered subsequently, with a summary of the WFI and UVS design and capabilities in Section 6.3. The WFI and UVS instruments have not been designed to the level of detail of the PIAAC instrument, as noted in Section 1.0.

3.4 PIAAC Instrument Interface to OTA

The total spectral range is 200–1200 nm (TBR), split into four spectral sub-channels.

The mirror labels (M1 – M4) are indicated in Figure 3.1-1. A narrow FOV is extracted at the fold mirror M3 (the central hole in M3 delivers light to the coronagraph instrument while the rest of the field is reflected to M4 for wide-field imaging) or, preferably, with a smaller mirror in the telescope aberrated focal plane. In the first scheme, the size of the hole is approximately 3 arcmin diameter (5% of the full FOV) in the optical design considered, and is a function of the distance between the telescope aberrated focal plane and M3. The optical design and packaging can be modified to minimize this distance if the resulting loss in FOV is scientifically too costly for general astrophysics.

At the coronagraph input, an aspheric mirror will correct the aberrated wavefront over a very narrow FOV (< 1 arcsec). This correction can be included within the prescription of the aspheric PIAA mirrors, therefore requiring no additional aspheric optics. Thanks to extensive use of dichroics, the instrument design combines exoplanet detection and spectroscopy in a single observing mode. The currently proposed number of spectral channels (16) can be increased due to higher SNR from the large PM. This modification can be achieved at the back end of the instrument by including

more dichroics, or by implementing an integral field unit (IFU) design. Given the small instrument FOV, this upgrade will not significantly increase the instrument volume and mass.

The OTA metering structure supports the PM, SM, and SI assembly. The PIAAC SI assembly consists of post-SM optics, including the PIAA mirrors, dichroic filters, deformable mirrors, BandICam bandpass filters, position-adjustable focal plane occulters, inverse-PIAA mirrors, detectors, and phase diversity sensors. The PIAA assembly attaches kinematically to the OTA metering structure. All electronics are located within the spacecraft.

3.5 PIAAC Instrument Summary

The PIAAC instrument has been described in detail in the PECO white paper (Guyon et al, 2008). Only a brief summary of the capabilities is given here.

WFCT takes advantage of the most powerful concept for suppression of diffracted starlight, PIAA, which enables 10^{-10} level, high contrast imaging, at a very close IWA of 2 λ/D. Unlike conventional coronagraph methods, the suppression is accomplished with very little loss of the planet flux, image sharpness, or the full angular field around the star, and promises greater efficiency than previous mission concepts.

The requirements for strong diffraction suppression and small IWA conflict when using conventional apodization or coronagraphic methods. The PIAA method redistributes the starlight via a lossless optical relay, producing a sharply focused star image that can be subsequently blocked by a stop, with very little starlight transmitted to the diffraction rings (10^{-10} contrast). Most of the light from planets with IWA > 2 λ/D passes the stop and can then be reformed into a true image by a second relay, which restores the original pupil distribution at unit magnification.

PIAA requires very accurate closed-loop control of wave front errors (WFE), especially low-order terms that diffract light into the 2-5 λ/D region. Deformable mirrors (DMs) are placed in each of four broadband channels, split out by dichroics after the PIAA unit. The WFC data is derived from the same 16-channel photon counting CCD camera that records the science data.

Very low vibration levels (~1 mas) are key to instrument operation. To achieve the necessary level, the Optical Telescope Assembly (OTA) will link to the spacecraft via the Lockheed Martin magnetic Disturbance Free Payload (DFP) system, which is described in Section 4.1 below.

The Ames Coronagraph Testbed (Belikov et al, 2009 a, b) is designed for flexible and rapid testing of PIAA and related technologies prior to full performance verification in vacuum at a facility such as JPL's High Contrast Imaging Testbed, or HCIT (Trauger et al, 2004). It began operations in March 2008 and has achieved $7x10^{-8}$ contrast at 2 λ/D in monochromatic light with the PIAA coronagraph (Figure 3.5-1). It is a successor to the first PIAA testbed at Subaru (Guyon, 2009), and is designed with several improvements from lessons learned there, particularly with regard to stability and flexibility. It is operated in a thermally stabilized air environment to make accessing and reconfiguring the layout easier and cheaper, complementing the HCIT at JPL.

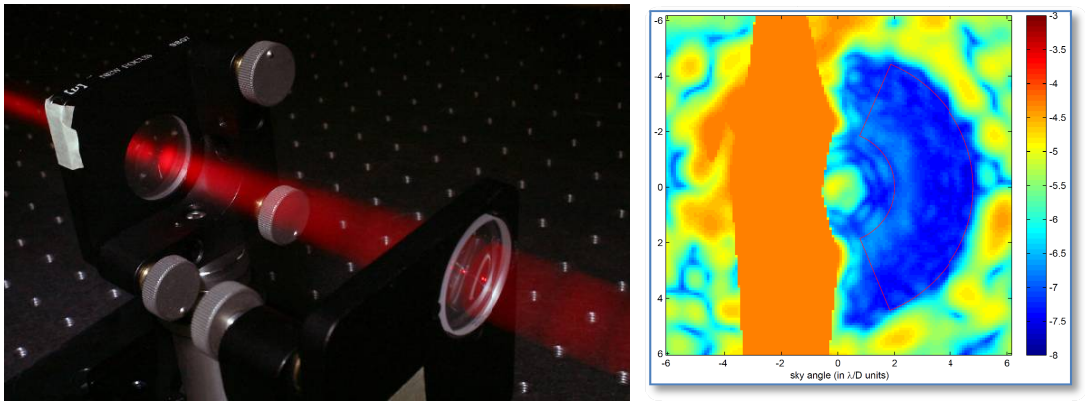

Figure 3.5-1. Left: the refractive PIAA system showing the remapping of a uniformly illuminated beam into a high-contrast apodization. Right: High contrast image taken at the Ames testbed, showing 7e-8 contrast between 2.0 and 4.8 l/D in the dark zone.

The current optical layout of the Ames testbed is shown in Figure 3.5-2. The light source is currently a long-coherence-length 658 nm laser, coupled into a single mode fiber. The single-mode fiber output serves as a reasonable approximation to a star. This light is then collimated by a 50-mm focal length lens into an almost uniformly illuminated beam, which passes through our refractive PIAA system, then gets reflected by our deformable mirror (made by Boston Micromachines). After the DM, light is focused onto a focal plane mask, and is reimaged onto the CCD. The PIAA system provides a PSF that is, in the absence of aberrations, completely concentrated within a radius of 2 λ/D (at 650nm) down to 10^{-10} contrast, and the focal plane mask is currently a binary disk occulter with a radius of 2 λ/D that blocks that PSF (with an optical density of 5). Two wavefront control algorithms are operating on our testbed, "Speckle Nulling" and "Electric Field Conjugation," (Trauger et al, 2004; Give'on et al, 2007).

Our layout is located inside an active thermal enclosure that has very recently started operating. It is currently being tuned, but already provides excellent stability of <1mK rms over ~ 1 hour.

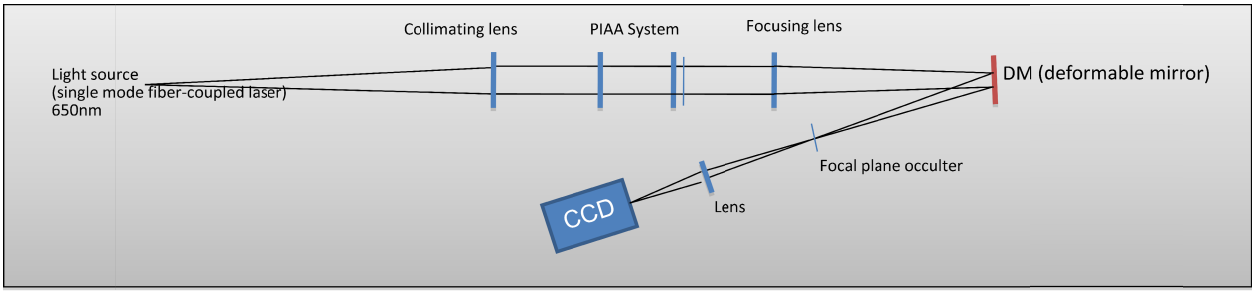

Figure 3.5-2. Default optical layout of the experiments on the Ames testbed.

3.6 WFI and UVS Instruments Summary

As in the case of THEIA, the WFI will be a dual-channel UV and optical (~120–1100 nm) imager. For WFCT it will cover the full 6 x 24 arc-minute FOV of the OTA. The channels will be separated by a dichroic beam splitter. Presently available detectors with 10-micron pixels are too large to match the 64-m focal length focus of the OTA. For 18 mas pixels on the sky, the detector pixels must be pitched at 5.6 microns. CMOS devices with even smaller pixels are made commercially, and the trend in the consumer market is toward ever smaller pixels. Thus space quality arrays at 5-micron pitch may be available in time for WFCT. If not, the OTA will be reoptimized with longer focal length to match the currently developed pixel sizes.

Again, as in the case of THEIA, it is expected that the vacuum UV instrument will share only the primary and secondary mirrors of the OTA. It will have relatively small field and will use small and dedicated relay and dispersive optics with fully optimized UV coatings. The far UV Spectrograph will target resolution of 30,000–100,000 in the 1000–3000 Å band.

3.7 WFCT Mission Spacecraft

The WFCT flight system is based on the Lockheed Martin–developed Spitzer spacecraft bus. The proven Spitzer spacecraft type design (in flight since August 2003) considerably reduces risk and cost to the WFCT program. The WFCT spacecraft will utilize the lightweight and low-cost electronics that are in the process of development.

3.8 Instrument Accommodation

The power distribution system provides redundant supply circuits for the SI. Separate heater circuits provide thermal control when the SI is off. A dedicated high-rate data interface is added between the SI and the communications subsystem. RS-422 channels support all other data interface requirements. Interface structure is placed on the spacecraft upper platform to mount the DFP system, which controls both the fine pointing and vibration isolation of the OTA. Thermal control is achieved through radiators, while the residual thermal effects to the OTA/SI system are minimized by the DFP and the active WFC system described above.

3.9 Spacecraft Design Requirements

High-contrast imaging places unique requirements on spacecraft stability and pointing accuracy. The pointing tolerance is ~1% of the PSF width (i.e., <1 mas). The WFCT strategy is: (1) operate in a stable orbit far from Earth; (2) derive accurate control signals from the bright target star image reflected by the coronagraphic stop, which drives a low-order

wave front sensor (LOWFS); and (3) eliminate vibration coupling from reaction wheels by utilizing the DFP. Another driving requirement is the thermal control of the primary mirror, with ~mK stability required.

The proven Spitzer spacecraft concept considerably reduces risk and cost: the spacecraft bus (TRL 8.5) is the most dimensionally stable in the industry, providing <1 arcsec 1-day stability using bus-mounted star trackers and gyros, thus avoiding mounting these components on the telescope focal plane.

The spacecraft design of major subsystems is shown in Table 3.9-1.

Table 3.9-1. Spacecraft design of major subsystems

Subsystem	Design Features
Structure	Modular octagonal Gr/CE composite with high stability payload interface, fixed solar panel
Mechanisms	Low shock deployment devices, focus mechanism on secondary mirror – internally redundant, low disturbance design FPO translation stage
Pointing Control	3-axis stabilized with wide-angle Sun sensors, star trackers, and inertial reference units for coarse pointing and contingencies. Instrument focal plane provides fine guidance during observations. Payload attitude control using DFP actuals with angle offload to spacecraft reaction wheels
Electrical Power	28±6 VDC fully solid-state direct energy transfer system. 16 Ahr Li ion battery, 26.8% efficiency improved triple-junction solar cell solar arrays
C&DH	Light, low power, block redundant RAD 750 design
Flight Software	Highly modular C/C++ open architecture based on extensive planetary observatory mission heritage, and COTS VxWorks OS
Comm	Laser communication, 2 Kbps uplink, 30 Mbps downlink at 0.6 Au
Thermal Control	Passive coatings with thermal blankets, constant conductance heat pipes, thermostatically controlled redundant heaters
Propulsion	Cold gas integral propellant management device

3.10 Pointing Control

The focal plane fine-pointing stability requirement is 1 mas. With a star of moderate brightness, the LOWFS achieves this precision at 100 Hertz. Pointing accuracy must always be better than 2 arcsec for LOWFS target acquisition. The key pointing stability requirement of <1mas is met using the DFP. This is readily attainable since HST achieves stability of 4 mas in a difficult low Earth orbit, viewing Earth's albedo essentially every orbit. HST has five flexible appendages and many operating mechanisms and meets 4 mas without the need for an articulating secondary mirror or fine steering mirror in the focal plane.

4. TECHNOLOGY DRIVERS

4.1 Disturbance Free payload, DFP, Vibration Isolation

The decoupling provided by the DFP (Pedreiro, 2002, 2003) provides the capability to meet the 1 mas requirement with margin. The DFP is a Lockheed Martin proprietary technology that has been developed over six years of internal research and development, and has currently achieved TRL 5/6. The DFP concept is based on a strict mechanical separation of the payload from the spacecraft, so that no mechanical load path exists for transmission of structural vibration. The DFP concept is shown in Figure 4.1-1.

The DFP method allows unprecedented payload isolation from spacecraft vibrations and simultaneous precision payload motion control. Non-contact actuators at the payload-to-spacecraft interface, which are commanded by error signals derived from either the LOWFS during fine pointing mode or by a payload inertial measurement unit, allow the payload to react against the mass of the spacecraft to precisely control angular line-of-sight. The limited stroke and gap of the interface actuators, with noncontact interface sensors, is then managed by control laws that command spacecraft inertial actuators, driving the spacecraft to follow the payload in inertial space.

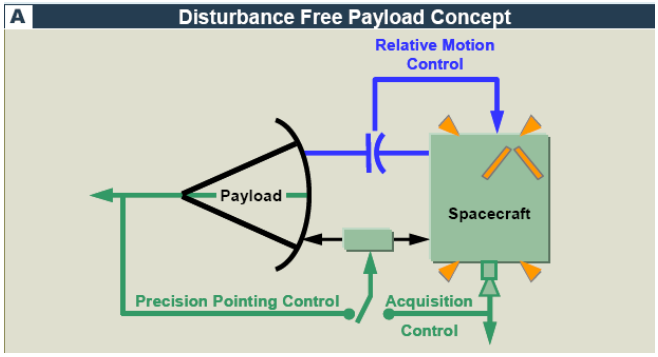

Figure 4.1-1. Lockheed Martin DFP Concept

Lockheed Martin has followed a comprehensive program of maturation of the DFP technology, encompassing modeling and simulation, component testing, integrated testing in a limited laboratory environment, and full, 6-DOF testing using realistic flight-like structures and control algorithms.

The DFP architecture brings several critical performance features to the WFCT mission. (1) Since DFP payload isolation occurs through mechanical separation, vibration isolation down to zero frequency is possible. The low-frequency stability requirements of the WFCT instrument makes isolation to zero frequency particularly important. (2) The non-contact interface sensors do not participate in payload inertial attitude control; thus, the payload attitude isolation performance is not limited by the noise characteristics of these sensors. (3) The mechanical separation of spacecraft and payload implies that requirements on structural stiffness and damping of spacecraft structure and disturbance sources (such as reaction wheels) can be significantly relaxed, leading to reduced spacecraft development cost. (4) The mechanical separation of spacecraft and payload on-orbit allows for greater flexibility for integration and testing of the WFCT system, since payload performance is largely independent of the structural response of the host spacecraft .

The DFP testbed (Dewell, Pedreiro et al, 2005) shown in Figure 4.1-2 has demonstrated over 60-dB broadband spacecraft-to-payload isolation, and extensive thermal-vacuum testing has been performed on DFP non-contact actuators and interface cables to ensure that the testbed accurately reflects flight conditions.

4.2 Precision Temperature Control

Analytical prediction of transient temperature response with mK accuracy has been verified by test with a 33.5-cm Pyrex mirror subject to small thermal perturbations that induce steady-state temperature gradients of 10–100 mK. Figure 4.2-1 shows the overall test configuration. The plano mirror was coated with protected silver on the front side and covered with MLI on the back and edges. A Kapton film heater on the back was used to induce step function heat loads on the mirror. Embedded PRTs, calibrated to ±1 mK over 15-40°C, provided axial and radial temperature data. Figure 4.2-2 shows the transient axial gradient at the edge. A finite element thermal model for test correlation was generated in I-DEAS/TMG. Test data were used for surface optical properties and MLI effective emittance estimates. Thermal balance test data were used to adjust the model parameters, and the model was then used to predict the transient through-thickness gradient response. Although the absolute gradient values differed by 25–40 mK, the transient prediction matched the data within approximately ±1 mK (Pecson, Hashemi, et al, 2002).

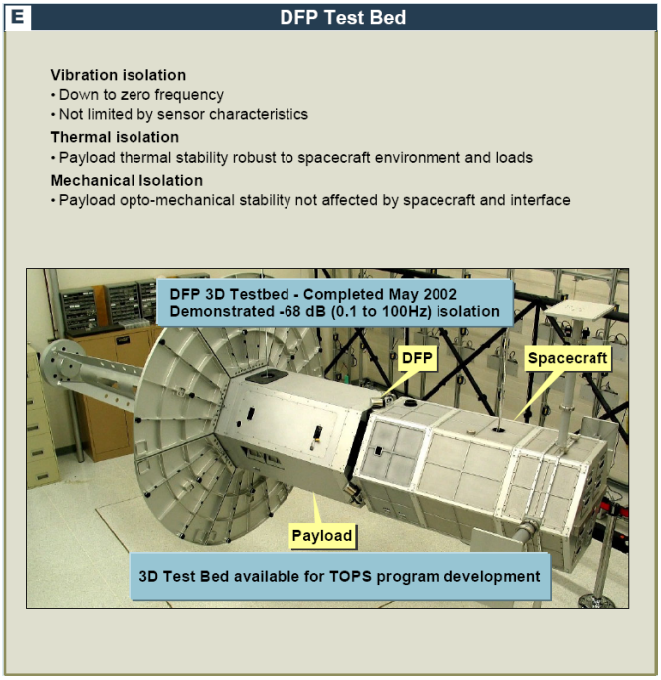

Figure 4.1-2. Lockheed Martin DFP Testbed

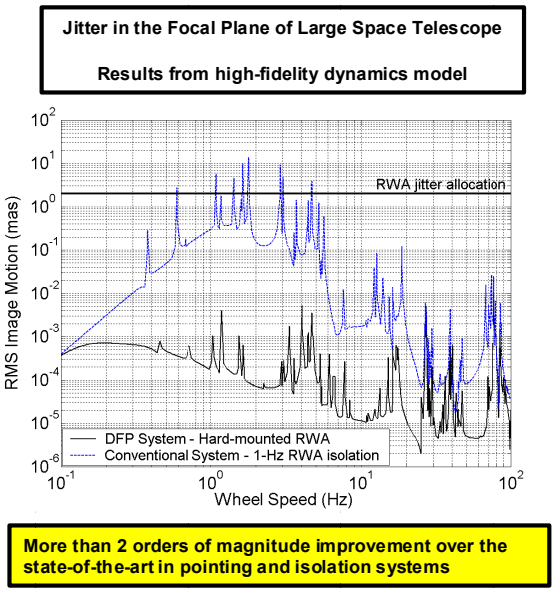

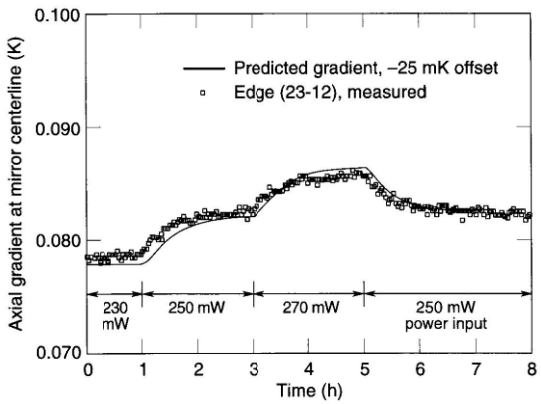

Figure 4.2-1. Overall test configuration

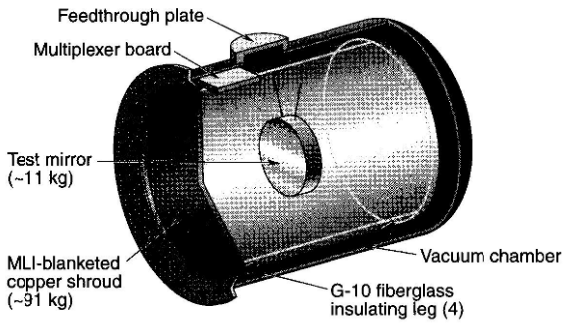

Figure 4.2-2. Edge gradient for step power changes

4.3 Deep-Space Laser Communications

Optical (laser) communications systems transmit data using the visible and near-infrared wavelength bands. WFCT can use such a system to transmit very high data rates, provided the system provides enough power to the receiver. In addition, optical-communications systems consume less mass, volume, and power than similar RF systems.

MIT Lincoln Laboratory is developing a laser communications system that will demonstrate high-data-rate communications between a lunar-orbiting NASA satellite and a ground site. The Lunar Laser Communications Demonstration (LLCD) will address NASA's need for very-high-rate, very-long-distance communications systems that are small enough to fly in space. The laser module is shown in Figure 4.3-1.

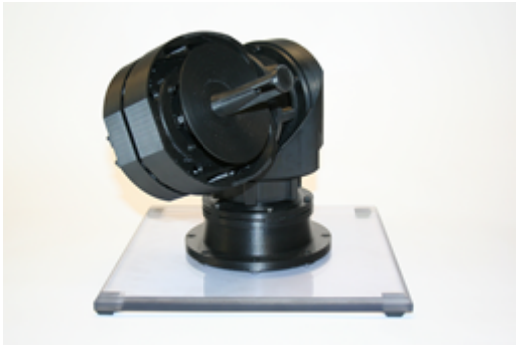

Figure 4.3-1. LLCD laser module model

The LLCD goal is to demonstrate transmission of over 600 megabits per second (Mbs) using a 4-inch telescope and a 1/2-watt laser installed on the lunar-orbiting satellite. The ground receiver will be nearly 10 times more efficient than any optical receiver ever demonstrated at these high rates. It will incorporate a pair of two-foot-diameter telescopes, each with its own very-high-performance light detector based on superconducting technology.

The Lincoln Laboratory–built LLCD space terminal will be carried on a NASA technology demonstration and science mission spacecraft named the Lunar Atmosphere and Dust Environment Explorer (LADEE), which is planned to launch in late 2011.

Another planned laser communications demonstration mission is the Mars Laser Communications Demonstrator, planned for launch on the Mars Telecom Orbiter in 2011, with an anticipated data rate of 10 Mbs.

Using the LLCD data rate of ~600 Mbs and assuming a linear relationship between the maximum data rate and the transmission distance (~20 times the LLCD distance at 0.6 AU), the WFCT Observatory at a maximum orbital distance of 0.6 Au could be expected to transmit at ~600 / 20 = 30 Mbs.

4.4 Large Telescope Optics

The WFCT PM is a 4-m on-axis monolith with an areal density of 50 kg/m2 and less than 15 nm of wavefront error (rms). Hubble's PM is a 2.4-m on-axis monolith with an areal density of 160 kg/m^2 and about 20 nm of rms wavefront errors. By this comparison the PM appears to represent a large technological challenge. However, since the Hubble PM was fabricated, significant advancements have been made in the areas of mirror design, fabrication, and polishing that significantly reduce technology risk, and essentially turn the task of fabricating the THEIA PM from one of pure technology development to one of a challenging engineering exercise.

These existing developments include: (1) abrasive water jet (AWJ) cutting to aggressively lightweight a mirror's core, (2) the invention of low-temperature fused (LTF) Corning ULE® mirror blanks; (3) segmented core fabrication that reduces manufacturing time and risk of breaking a full-sized fragile core, (4) pocket-milled facesheets that significantly reduce overall mirror weight, (5) computer-controlled active laps polishing of highly aspheric optics, (6) the combination of pocket-milling and deep segmented AWJ cores, and (7) technology advancement in optic and telescope metrology.

Many of these new processes have already been employed on existing programs such as Ikonos, Nextview, AMSD, TDM, and AFRL DOT. Nevertheless, because the WFCT PM is large, relatively expensive, and not completely without risk, the WFCT plan is to develop a subscale prototype to demonstrate all processes prior to entering Phase C. A subscale polishing demonstration will be used to confirm that the PM smoothness requirements could be met on a mirror of comparable stiffness.

Development of a full-scale blank was also considered but deemed not necessary by our study partner, ITT Space Systems Division of LLC. Rather, a proto-flight unit will be used to qualify the design, as is the case for most of the optical systems developed by ITT. Witness samples will be processed in parallel with the flight unit and certified by optical inspectors at multiple points in the process.

There are other mirror technologies that could be developed that could lessen the risk, cost, and schedule for the WFPC PM, but they are not deemed essential. These include: (1) ULE® welding could enable a large blank to be built up from smaller pieces. (2) ULE® large boule development would reduce the schedule required to produce all of the glass

required for large monolithic mirrors. (3) ULE® striae (visibly detectable layers in the glass) are developed as a result of non-uniformities in the distribution of titanium oxide molecules that are introduced into the material to minimize the materials coefficient of thermal expansion. When ULE® is polished, the non-uniformities in the striae layers can result in high spatial frequency surface errors that could adversely impact the system performance of a telescope.

5. OBSERVATORY I&T FLOW

The observatory I&T sequence includes OTA, SI, and spacecraft post-delivery checkout, mechanical mating, alignment, ambient functional, deployment, RF compatibility, mission simulation, launch rehearsal, and environmental tests including EMC, vibration, acoustic and thermal vacuum, and thermal balance. To ensure system compatibility, ground station interfaces are validated at the spacecraft level prior to the observatory testing. End-to-end mission simulation testing is conducted at Lockheed Martin in Denver to reduce on-orbit operational risk.

6. COST ESTIMATE & SCHEDULE

The WFPC total mission cost is estimated to be $4.2B in FY 2009 dollars. That sum includes launch services at $220M.

The cost of the WFI, UVS, management, system engineering mission design, spacecraft, system I&T and mission, science and science data center, ground system, and EPO was offered by THEIA and gratefully accepted. <Please check punctuation--meaning is unclear.>

Our cost is $800M less than THEIA (Kasdin, 2009) because it does not need an occulter/ spacecraft/launch vehicle.

The cost estimate and program schedule appear below.

Cost Estimate	$M
Pre-Phase A Mission Concept	15
Total Technology Development	140
PIAAC	40
Primary Mirror (off axis)	60
Detector	40
Management, Sys Engr. Mission design & Mission	140
Science & Science Data Center	250
PL System	2100
WFI	400
UV	200
PIAA	100
Telescope	1400
Spacecraft Bus system	200
System Level I&T	100
Mission Ops & Grd Data System	130
EPO	35
Reserve (30%)	900
Launch Service	220
Total Mission	**4230**

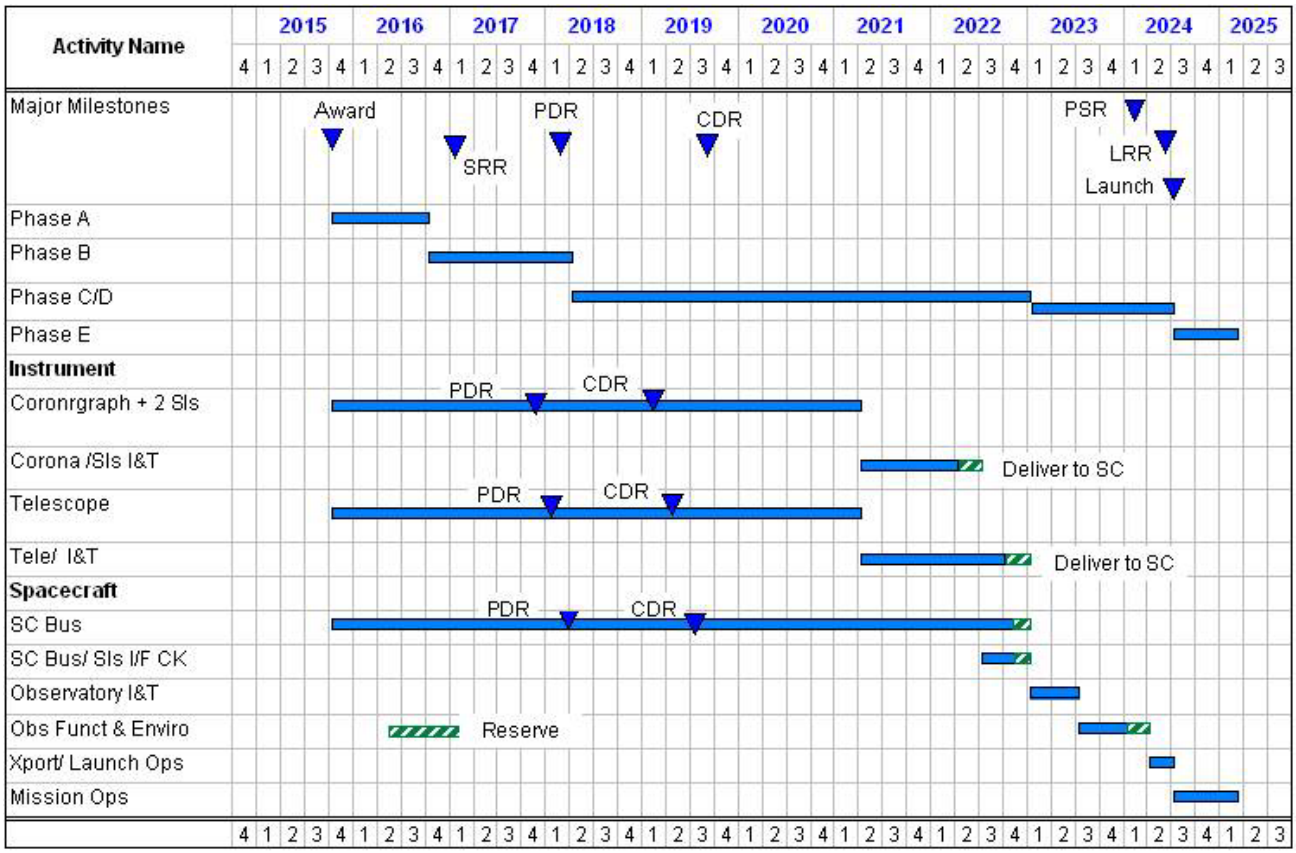

The launch of the WFCT in the 2024 timeframe is important for astronomy. At that time (2024), the operation of both HST and Spitzer will have ceased. JWST will be approximately ten years in orbit (it is designed for five years with a ten-year goal), hence the launch of WFCT continues the outstanding astrophysics science of HST and carries out significant exoplanet science. The WFCT mission meets the requirements of the 2000 Decadal committee, which stipulated that a flagship exoplanet mission must also do important astrophysics science.

REFERENCES

Belikov, R., et al, 2009.a, *Proc SPIE* 08/2009, *in prep.*

Belikov, R., et al 2009.b, *Proc SPIE 7440*, 08/2009.
Bradac, M., et al, 2006, ApJ, 652, 937
Clampin, M., 2002, http://www.stsci.edu/stsci/meetings/space_detectors/pdf/clampin.pdf
Clowe, D., et al, 2006, ApJL, 648, 108
Dalcanton, J.J., et al, 2009, submitted to ApJS
Dewell, L., Pedreiro, N., et al, 2005, SPIE Paper No. 5899, July 2005.
Dey, A., et al, 2005, ApJ, 629, 654
Fardal, M., et al, 2001, ApJ, 562, 605
Francis, P.J., et al, 2001, ApJ, 554, 1001
Give'on A., et al, 2007, *Optics Express*, Vol. 15, Iss. 19, pp. 12338-12343, 09/2007
Guyon O., 2003, A&A, Vol. 404, pp. 379-387
Guyon O., et al 2008, SPIE, Vol. 7010, 70101Y
Guyon O., 2009, *PASP*, Vol 122, Iss 887, pp. 71-84
Guyon O., Shao, M., Shaklan, S., et al, 2010, SPIE, San Diego, Calif., 7731-83
Haiman, Z., et al, 2000, ApJL, 537, L5
Harris, J., & Zaritsky, D. 2004, AJ, 127, 1531
Heap, S., et al, 2009, Tech. White Paper for Electromagnetic Observations from Space
Ibata, R., et al, 2007, ApJ, 671, 1591
Kasdin J., 2009, Exoplanet Forum, Pasadena, CA
Keel, W., et al, 1999, AJ, 118, 2547
Keres, D. et al, 2005, MNRAS, 363, 2
Munoz, R.R., et al, 2006, ApJ, 649, 201
Pecson, J., Hashemi, A., et al 2002, *Spacecraft Thermal Control Handbook*, Editor, David G. Gilmore, pp 639-655.
Pedreiro, N., et al, August 2002 AIAA Paper No. 5027
Pedreiro, N., Journal of Guidance, Control, and Dynamics, V. 26, No. 5, Sept/Oct 2003, pp. 794-804.
Steidel, C. C., et al, 2000, ApJ, 532, 170
Taniguchi, Y., & Shioya, Y. 2000, ApJL, 532, L13
Trauger, J., et al, 2004, *Proc. Of SPIE* 5487, 1330-1336.
Yang, Y. et al, 2009, ApJ, 693, 1579